EARTH Interactions

Copyright © 2008, Paper 12-005; 4,269 words, 7 Figures, 0 Animations, 1 Table.
http://EarthInteractions.org

Diurnal to Annual Precipitation Sensitivity to Convective and Land Surface Schemes

Alex C. Ruane*

Oak Ridge Associated Universities/National Aeronautics and Space Administration Postdoctoral Program, NASA Goddard Institute for Space Studies, New York, New York, and Experimental Climate Prediction Center, Scripps Institution of Oceanography, University of California, San Diego, La Jolla, California

John O. Roads

Experimental Climate Prediction Center, Scripps Institution of Oceanography, University of California, San Diego, La Jolla, California

Received 10 December 2007; accepted 13 February 2008

ABSTRACT: Precipitation's diurnal to annual variance distribution and atmospheric water cycle component interactions are examined globally for sensitivity to convective and land surface schemes. The main regional features of statistics identified in previous reanalyses are robust in unconstrained continuous simulations corresponding to the reanalyses' convective and land surface schemes. A change from the simplified Arakawa–Schubert (SAS) to the relaxed Arakawa–Schubert (RAS) convection scheme reorganizes the variance of rainfall at low latitudes to a redder spectrum. Despite the potential increase in soil moisture memory, a change from the Oregon State University (OSU2) to the Noah land surface model does not noticeably affect the variance distribution of precipitation. The competition between dynamic and thermodynamic

* Corresponding author address: Alex C. Ruane, NASA Goddard Institute for Space Studies, 2880 Broadway, New York, NY, 10025.
E-mail address: aruane@giss.nasa.gov

DOI: 10.1175/2008EI256.1

sources of precipitation's variability is affected by the choice of both the land surface model and the convective scheme. Noah reduces evaporation's role over land, with vapor convergence compensating, while RAS/SAS sensitivities result in complex regional redistributions of component covariance.

KEYWORDS: Precipitation; Convection; Land-surface model

1. Introduction

Convective and land surface parameterizations (and the ways in which models interact with these schemes) play a large role in atmospheric water cycle simulations. These parameterizations have been refined to produce reasonable mean precipitation across the globe at seasonal and interannual time scales, but an improved representation of the higher-frequency manner in which this precipitation falls is still required to fully understand extreme events (Trenberth et al. 2003). Ruane and Roads (Ruane and Roads 2007b, hereafter RR2007b; Ruane and Roads 2008, hereafter RR2008) presented analysis methods that isolate different temporal characteristics of precipitation, and these statistics' sensitivities to model parameters and reanalyzed data assimilation are the focus of this work.

Ruane and Roads (RR2007b) examined the variance distribution of precipitation in observation-based high-resolution precipitation products and two global reanalyses. Spectral decompositions of three years of 3-hourly precipitation records were divided into six variance categories, which together captured the entire diurnal to annual variance. Precipitation featured disproportionately high variance at lower frequencies in all global sets, characterizing a "red" spectrum (Gilman et al. 1963). Significant biases were identified in the reanalyses, however, including a large redistribution of variance from higher to lower frequencies that caused one of the reanalyses to be reddened further. RR2007b attributed this shift to the reanalyses' convection schemes, but the sensitivity experiments conducted here were required to fully isolate the convective and land surface effects from other reanalysis differences.

Interactions between components of the atmospheric cycle on several intraseasonal time scales were then explored by Ruane and Roads (RR2008). The atmospheric water budget (balancing precipitable water tendency with exported precipitation and moisture imported by evaporation and vapor flux convergence) was decomposed into its mean and transient parts, completely describing the variance of any budget component through its normalized covariance with the other components. For example, the variance of precipitation may be described through

$$\frac{\mathrm{cov}(P', P')}{\mathrm{var}(P')} \times 100\% = \frac{\mathrm{cov}(E', P') + \mathrm{cov}(-T', P') + \mathrm{cov}(C', P')}{\mathrm{var}(P')} \times 100\% = 100\%, \tag{1}$$

where P is precipitation, E is evaporation, T is the precipitable water tendency, C is the vertically integrated vapor flux convergence, and P' indicates the transient component of P on a given time scale. RR2008 discussed the regional patterns described by the central portion of Equation (1) applied to a reanalysis system, but

suggested that data assimilation and the selection of parameterization schemes must have had an influence on the simulated interactions of the water cycle.

The atmospheric water cycle has been the focus of many reanalysis evaluations (Roads et al. 1994, 2002; Trenberth and Guillemot 1998). The sensitivities of mean water cycle components to convective (Meinke et al. 2007) and land surface (Kato et al. 2007) parameterizations, as well as contrasts between continuous experiments and those with reanalyzed data assimilation (Roads et al. 1999; Nigam and Ruiz-Barradas 2006), have been the subject of previous work. This study will focus instead on the sensitivity of the RR2007b and RR2008 higher-frequency temporal statistics. Section 2 describes long-range continuous simulations conducted for this investigation in a manner similar to the Atmospheric Model Intercomparison Project (Gates et al. 1999), and section 3 compares their temporal characteristics to our previous reanalysis studies. The variance effects of convective parameterizations and land surface models (LSMs) are examined in sections 4 and 5, respectively, and a brief summary and conclusions are presented in section 6.

2. Experiment design

Table 1 provides an overview of the six simulations examined in this study, which are described in this section. As part of the contribution of the Experimental Climate Prediction Center (ECPC) to the Coordinated Enhanced Observing Period (CEOP, now called the Coordinated Energy and Water Cycle Observations Project; Koike 2004; Lawford et al. 2006), the National Centers for Environmental Prediction (NCEP)–Department of Energy Reanalysis-2 (R2; Kanamitsu et al. 2002b) and a corresponding enhanced reanalysis using the NCEP–ECPC Seasonal Forecast Model (SFM; Kanamitsu et al. 2002a) in place of the R2 model were produced for the 2002–04 CEOP period. Ruane and Roads (Ruane and Roads 2007a) provide a more complete description of these reanalyses. Both reanalyses utilize the same data assimilation system (and input data) but have underlying global spectral models that employ different convective and land surface schemes. The SFM reanalysis uses the relaxed Arakawa–Schubert convective scheme (RAS; Moorthi and Suarez 1992) and the Noah LSM (Ek et al. 2003). The R2 uses alternate (but earlier) versions of these schemes: the simplified Arakawa–Schubert convective scheme (SAS; Pan and Wu 1995) and the second Oregon State University LSM (OSU2; Pan and Mahrt 1987). Briefly, RAS is different from SAS in that it "relaxes" toward a climatological atmospheric profile each time the parameterization is invoked. Noah is notable for having vertical layers of 0–10, 10–40,

Table 1. Overview of experiment type, whether or not data assimilation was employed, and the physical packages used in the six simulations examined in this study.

Expt	Type	Data Assimilation	Convection	Land surface
R2	Reanalysis	4 times daily	SAS	OSU2
SFM	Reanalysis	4 times daily	RAS	Noah
SO	Continuous	None	SAS	OSU2
SN	Continuous	None	SAS	Noah
RO	Continuous	None	RAS	OSU2
RN	Continuous	None	RAS	Noah

40–100, and 100–200 cm, while OSU2 combines these bottom layers into a single 10–200-cm layer.

Four long-range continuous simulations forced by reanalysis SST were also carried out; two containing the same convective and land surface schemes as the reanalyses (RN, utilizing RAS and the Noah LSM like the SFM; and SO, employing SAS and the OSU2 LSM like the R2), and two containing the other possible combinations of these schemes (RO, utilizing RAS and the OSU2 LSM; and SN, utilizing SAS and the Noah LSM). Other than their parameterization options, these continuous experiments had identical model code from the 5 January 2007 Concurrent Version System (CVS) version of the SFM. Each simulation was initialized from the reanalysis containing its compatible LSM, and produced 3-hourly output from 2000–06. Excluding the first year to remove most spinup effects, the RR2007b and RR2008 statistical analyses were repeated for the 2001–06 period (twice the length of the reanalysis period originally examined for CEOP, allowing for more realizations of the longer time scales).

3. Reanalyses and continuous runs

Before we compared these continuous simulations, we first checked them against the baseline established by the reanalyses. The diurnal to annual precipitation characteristics described previously in RR2007b and RR2008 are a reflection of both the atmospheric model and the data assimilation components of the reanalysis system, but analysis of these continuous simulations allows us to isolate the atmospheric model portion. The variance distribution of precipitation from the RN experiment is shown in Figure 1 (comparable to Figure 9 examining the SFM in RR2007b), featuring a red spectrum with regional shifts in variance due to the Hadley circulation, monsoons, mountains, coastlines, and warm sea surface temperatures that are attributes of all experiments. The RN also contains a unique (additional) reddening of the tropical spectrum that was also a characteristic of the SFM reanalysis.

The data assimilation system does have several noteworthy effects, however. The stark contrast in precipitation's annual variance distribution between the tropics and the extratropics in the SFM reanalysis is lessened in the continuous RN simulation (Figure 2a), with the highly convective intertropical convergence zone and Southeast Asian monsoon regions experiencing less annual variance and the extratropical continents displaying a larger annual signal. The diurnal variance category displays a similar moderation (not shown), where the prominent tropical variance in the SFM is reduced and diurnal variance over the extratropical continents increases. A similar geographical pattern shows adjustment in the opposite direction in the high-frequency (6–36 h) portion of the spectrum (Figure 2b), where variance plays a larger role over tropical oceans and has reduced influence over the continents. These shifts are not enough to change the "red" nature of precipitation's spectrum.

The main features describing precipitation's annual, intraseasonal (defined for normalized covariance as the 7- to ~80-day period), and diurnal variance through its normalized covariance with evaporation, negative precipitable water tendency, and vertically integrated vapor flux convergence are common to all experiments (Figure 3 shows the SO experiment to facilitate comparisons to RR2008's R2

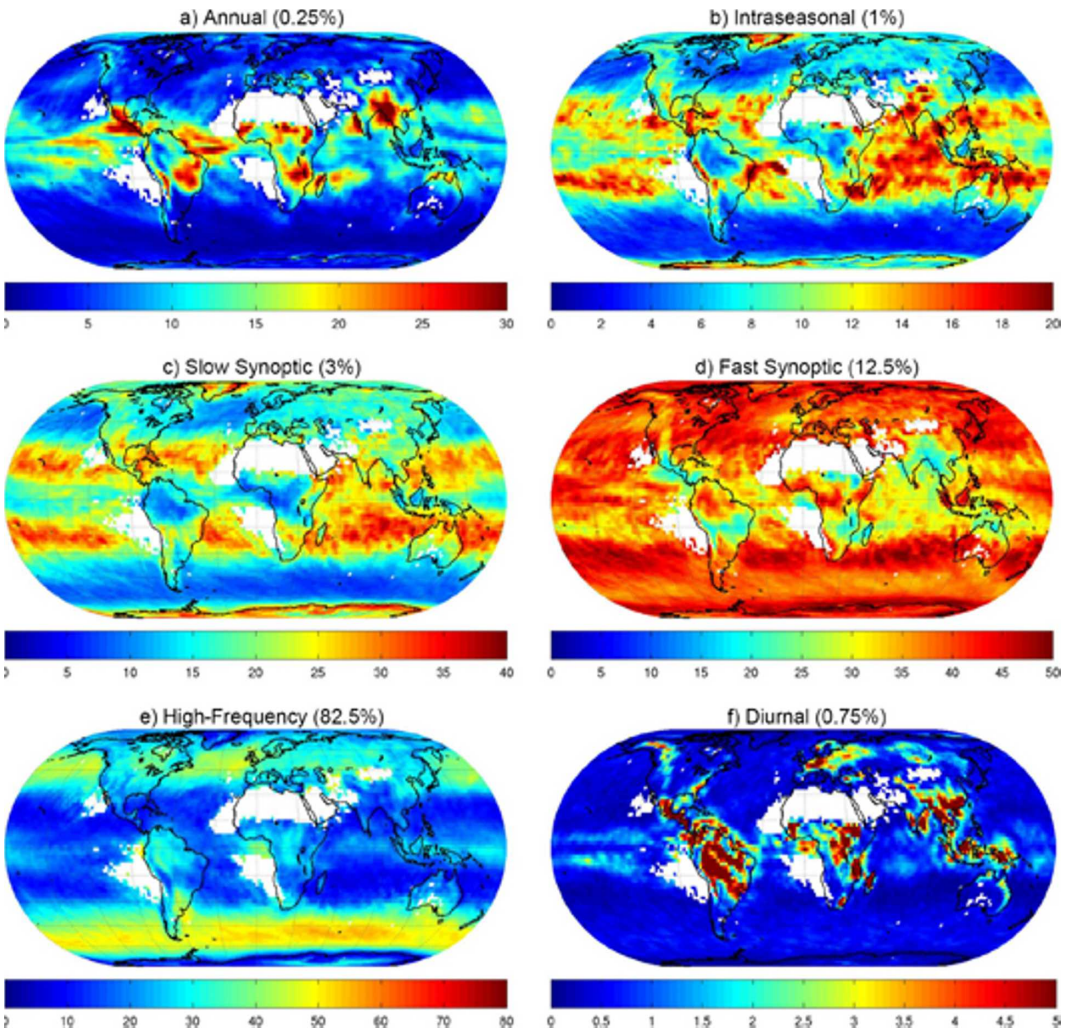

Figure 1. Percentage of precipitation's variance contained in the (a) annual (~80 days–1 yr), (b) intraseasonal (20 to ~80 days), (c) slow synoptic (6–20 days), (d) fast synoptic (36 h–6 days), (e) high-frequency (6–36 h), and (f) diurnal (24-, 12-, 8-, and 6-h windows) for the RN experiment. The percentage of total variance bands in each category is also presented.

characteristics). Annual rainfall covaries with advected land (thermodynamically driven) and marine (dynamically driven) air masses in the extratropics while the tropics are dynamically controlled. Dynamic convergence also dominates the intraseasonal frequencies that lack coincident external solar forcing. Evaporation drives the diurnal water cycle over most land areas, although vapor convergence plays a significant role over the tropics. Together, the variance distribution and water cycle interactions associated with precipitation are very similar between reanalyses and continuous simulations, indicating a limited role for data assimilation in determining these statistics.

The continuous simulations have a larger interannual range in normalized co-

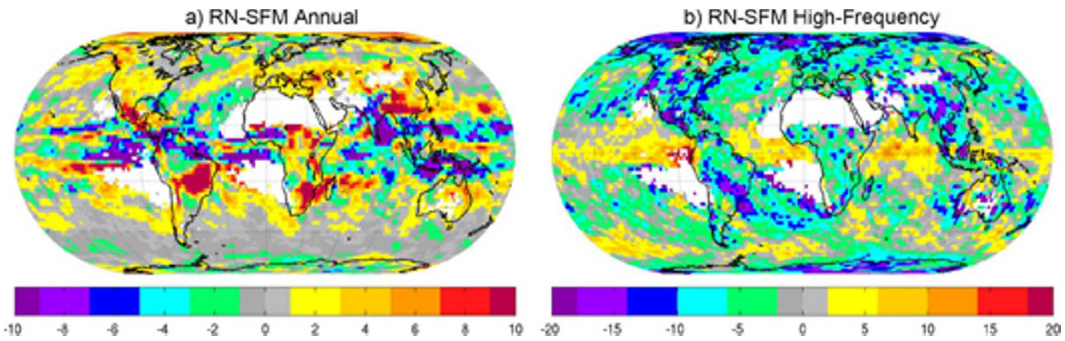

Figure 2. RN–SFM differences in the percentage of precipitation's variance contained in the (a) annual and (b) high-frequency variance categories.

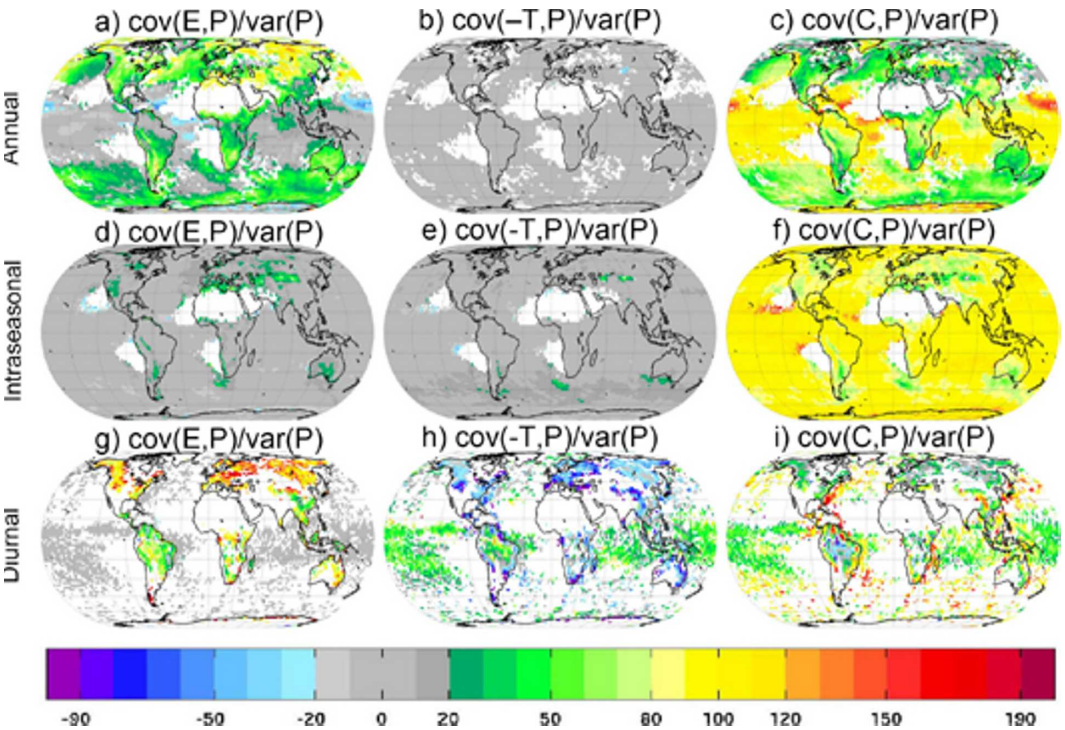

Figure 3. Normalized covariances (%; based on Equation (1); see RR2008) describing the comprehensive variance of precipitation through its covariance with (a), (d), (g) evaporation; (b), (e), (h) negative precipitable water tendency; and (c), (f), (i) vertically integrated vapor flux convergence for the SO experiment at annual (a)–(c), intraseasonal (d)–(f), and diurnal time scales (g)–(i). Normalized covariances of 0% indicate no covariant relationship, 100% indicates covariance of the same magnitude and phase, >100% indicates that the variable examined varies in phase with precipitation but with a higher magnitude, and <0% indicates a covariant relationship that is of opposite phase. White areas were omitted because of large interannual ranges.

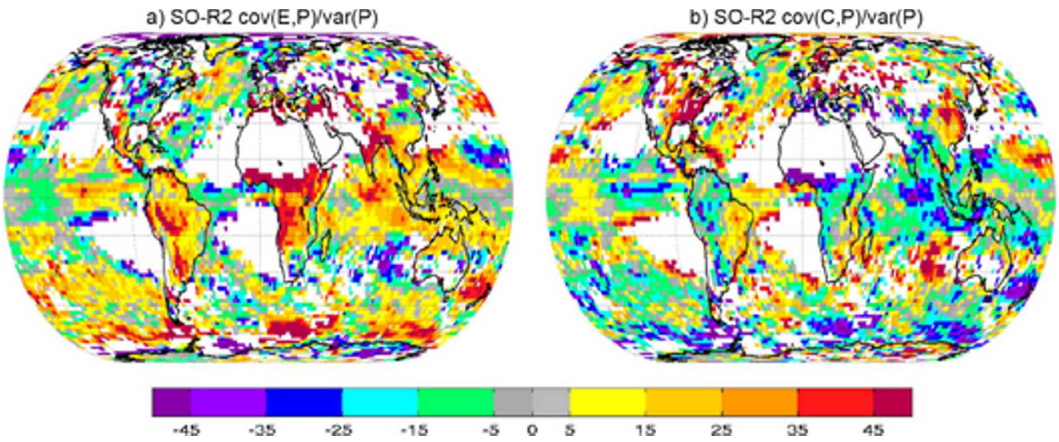

Figure 4. SO–R2 annual normalized covariance differences describing the variance of precipitation through (a) evaporation and (b) vapor flux convergence.

variances describing diurnal precipitation, resulting in a higher number of grid locations that were omitted for inconsistent behavior (see Figures 3g–i). In part this is due to having twice as many years to compare, but also suggests that the 4-times-daily assimilation of observations introduces a more consistent diurnal variation than is produced in the continuous experiments. Whether this is a real diurnal variation or an aspect of precipitation spinup in the reanalyses (Betts et al. 1999) is not clear.

SO–R2 comparisons validate RR2008's separation of the R2's model increment (generated by the rapid reinitialization of the analysis with different column moisture profiles) and natural tendencies. Precipitable water tendencies had a negligible impact on the low-frequency variance of precipitation in the continuous experiments (not shown), but the normalized covariances of evaporation and convergence with precipitation are similar. Schubert and Chang (Schubert and Chang 1996) noted that model increment biases are dominated by errors in the evaporation field during the early spring and then by a combination of errors in the evaporation and precipitation fields during the late spring. Comparisons between the R2 and the SO indicate that areas experiencing large model increment biases at low frequencies in the R2 replace this variance with either enhanced evaporation or convergence influence, though neither dominates and the distribution across different regions is not uniform (Figure 4).

4. Convective scheme comparison

The sensitivity of precipitation's temporal characteristics to the relaxed and simplified Arakawa–Schubert convective schemes (RAS and SAS) is examined in this section by contrasting continuous simulations with different convective schemes and identical land surface models (RN–SN and RO–SO). As SAS has been replaced by RAS as the default scheme in ECPC's atmospheric models, the experiment with the SAS scheme will be considered the control run in these comparisons.

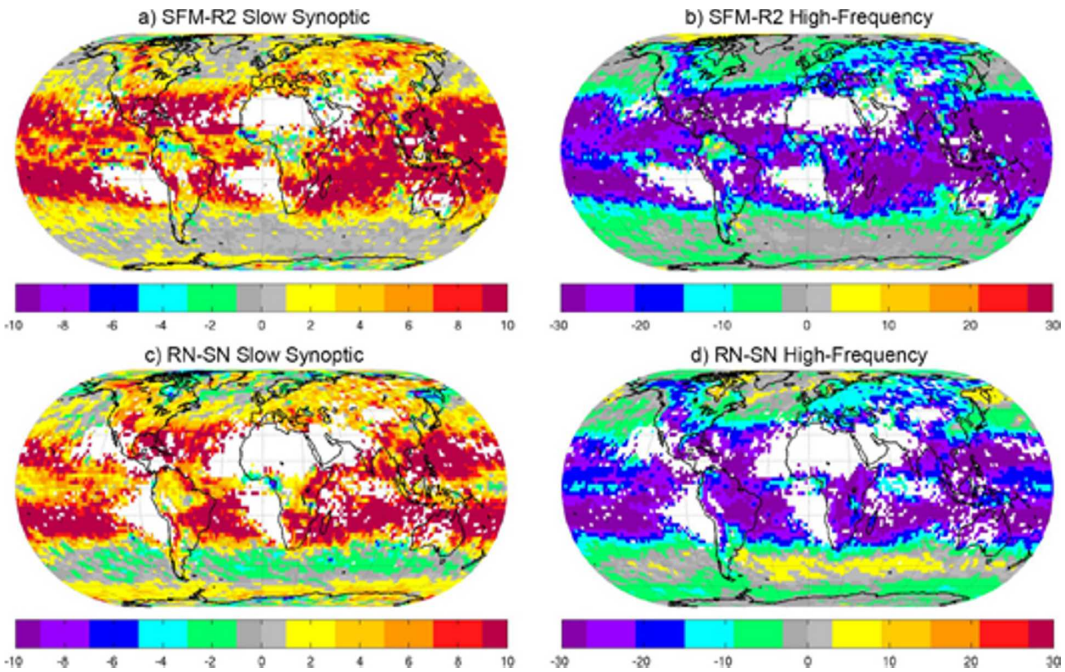

Figure 5. As in Figure 2, but for SFM–R2 (a) slow synoptic and (b) high-frequency variance categories and RN–SN (c) slow synoptic and (d) high-frequency variance categories.

A major finding of RR2007b was the significant reddening of the SFM reanalysis in comparison to the R2, which is best illustrated by the large shift in variance from the high-frequency category to lower-frequency bands (Figures 5a,b). RR2007b hypothesized that the significant spectral reddening in the SFM reanalysis was due to the RAS convection scheme's relaxation toward longer time scales in the SFM. The impact of the differing convective parameterizations could not be isolated, however, as the LSM, clouds, and longwave radiation schemes also differed from the R2.

The continuous experiments verify a clear sensitivity of a model's distribution of precipitation's variance to its convective parameterization. In comparison to the SAS scheme, the RAS convection scheme shifts a large portion of variance from higher to lower frequencies throughout the tropics (Figures 5c,d). Here we show the impact on the slow synoptic category, but similar trends are apparent at all periods longer than ~2 days. This characteristic pushes RAS schemes (whether paired with Noah or OSU2 LSMs) away from the observation-based spectra in RR2007b, which were less red in comparison. The similarities between Figures 5a,b and Figures 5c,d indicate that the spectral discrepancies between the R2 and the SFM is overwhelmingly attributable to their selection of convective parameterizations.

There does not appear to be any consistent geographical coherence between the variance changes and shifts in total precipitation between experiments. Accompanying the changes in precipitation, a similar reddening of the vapor convergence

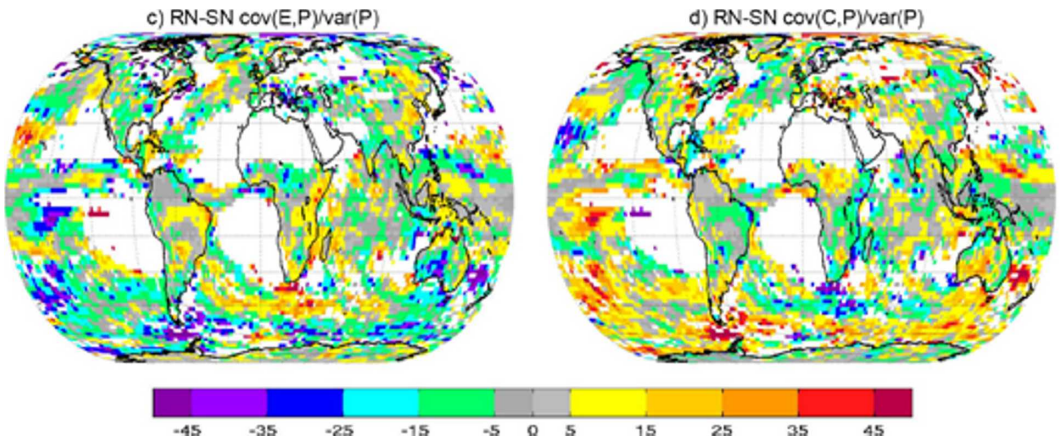

Figure 6. RN–SN annual normalized covariance differences describing the variance of precipitation through RN–SN (a) evaporation and (b) vapor flux convergence.

and precipitable water tendency variance spectra is also apparent when RAS is used (not shown).

The RN–SN differences in the normalized annual covariances describing precipitation are presented in Figure 6. As the variation of the precipitable water tendency term on these scales is negligible, reduction in evaporation's influence is directly counteracted by an increase in the role of vapor convergence over land. Overall, the dominant balances and exchanges between water cycle components are insensitive to RAS' redistribution of precipitation's tropical variance. There is geographical coherence, however, between the RN–SN and the RO–SO differences (not shown), suggesting a complex regional sensitivity that merits further investigation.

5. LSM comparison

The sensitivity of precipitation's temporal characteristics to land surface models (Noah and OSU2) is examined in this section by contrasting continuous simulations with each of these schemes and identical convective schemes (SN–SO and RN–RO). The OSU2 LSM was the basis for the Noah LSM, so OSU2 will be the control scheme in these comparisons. The sensitivity of precipitation to LSM depends on the differing triggers of the RAS and SAS convective parameterizations, but sensitivities discussed in this section are common to both the SN–SO and RN–RO comparisons.

In addition to LSMs' direct effect on the water cycle through evaporation parameterizations, the additional vertical layers of the Noah model could introduce additional time scales through enhanced resolution of soil moisture memory. Wu and Dickinson (Wu and Dickinson 2004) found that soil moisture anomalies persist for less than a month in the soil's upper 10 cm, but can last several years at the 2-m level. While the OSU2 LSM merges the 10-cm to 2-m anomalies into a long time scale, the Noah LSM can potentially resolve distinct anomalies at

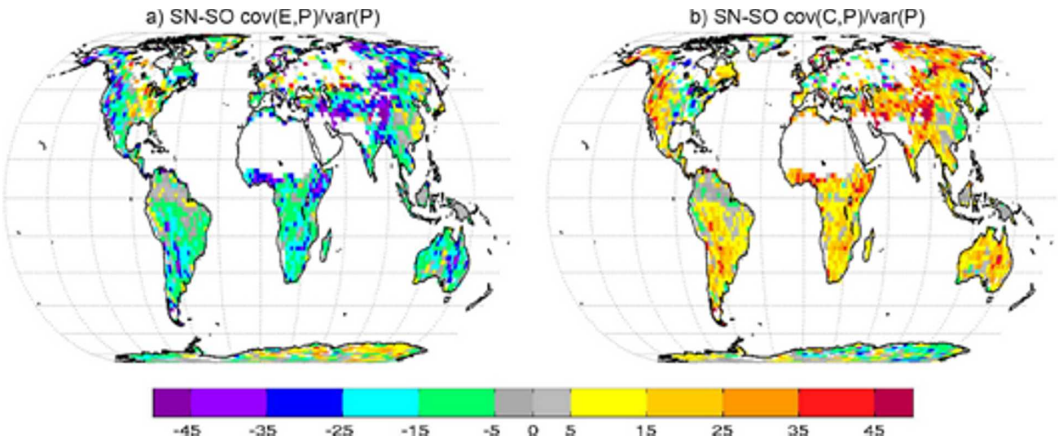

Figure 7. SN–SO annual normalized covariance differences describing the variance of precipitation over land through (a) evaporation and (b) vapor flux convergence.

intermediate depths between 10 and 100 cm that can last 1–10 months (Wu and Dickinson 2004).

Our sensitivity tests examined whether Noah's capacity for intermediate-depth soil moisture variability translated into a shift in precipitation's behavior. Compared to OSU2, however, Noah does not seem to enhance intraseasonal or annual precipitation variance in any consistent pattern (not shown). Precipitation's variance is not coherent with the variance of any single soil moisture level, indicating a disconnect between model precipitation and soil moisture anomalies. In fact, the selection of LSM in the continuous simulations does not have any significant effect on the variance distribution of precipitation that stands out from the background. Whether the minor interactions between rainfall and surface water processes are due to prohibitively weak surface variation or to convective parameterizations that are overwhelmingly tuned to other factors merits further investigation.

The LSMs do, however, affect the component interactions that lead to precipitation. The covariant relationships that govern regional precipitation variability are largely consistent for both the Noah and OSU2 LSMs, but models with the Noah scheme reduce the contribution of evaporation on annual (Figure 7) and intraseasonal time scales over most land areas. This could either be the result of a reduction in evaporation's variability or an increased phase shift between evaporation and precipitation that reduces covariation. As discussed in section 4, the evaporation and convergent terms feature equal and opposite interexperiment contrasts on long time scales. The geographical pattern of this bias is not shared by any variation in the mean evaporation, vapor convergence, or precipitation. Convective parameterizations often fail to capture anomalous regional variability by elevating local thermodynamics over the external influences that control a region through dynamic convergence, and this bias is apparently reduced in the Noah LSM.

6. Summary and conclusions

To gauge the sensitivity of precipitation's intraseasonal temporal characteristics to data assimilation, convective parameterization schemes, and LSMs, continuous simulations were run from 2000–06 featuring identical code but unique convective and LSM parameterization sets. Using the statistical methods in RR2007b, precipitation's intraseasonal variance is compared between continuous simulations and with reanalyses produced for the CEOP experiment. Similar comparisons also allow an exploration of water cycle component interactions that lead to precipitation at several time scales, as was done for the R2 in RR2008.

Overall, the temporal characteristics identified in RR2007b and RR2008 are quite robust in the continuous runs with corresponding convective and LSM schemes, suggesting that the diurnal to annual attributes of precipitation are features of the atmospheric model and are only slightly modified by the data assimilation component of the reanalysis system. The continuous runs lacked the reanalyses' more consistent diurnal cycle, however, and reduced the meridional gradient that caused such a stark contrast in precipitation's tropical and extratropical variance. The reanalyses' model increment bias is eliminated in the continuous simulations, causing a regional redistribution of low-frequency covariance to the evaporative and convergent components.

Adjusting from SAS to RAS leads to a strong reddening of the tropical spectrum, as the relaxation mechanism in RAS increases low-frequency variance at the expense of higher frequencies. Thus, RAS moves away from RR2007b's observation-based spectra in comparison to SAS. The mean precipitation comparisons do not show any similar geographical contrast, however, indicating that different parameterization sets produce similar rainfall totals despite unique temporal representations. Main features in the types of water cycle component interactions that lead to precipitation are consistent regardless of the convective parameterization used here, although complex geographical shifts occur to a minor extent.

The increased vertical resolution in the Noah LSM's soil column does not produce noteworthy increases in low-frequency precipitation through enhanced soil moisture memory interactions. Either the moisture anomalies are too weak to stand out from the background variability, or the convective parameterizations are dominated by other constraints. Instead, the Noah model reduces the (perhaps overbearing) local thermodynamic control over low-frequency precipitation, leading to an increased role for dynamic influences from neighboring regions.

This study has demonstrated the utility of continuous runs and the use of these temporal statistics for evaluating model performance. These examinations could be expanded to include other models, parameterization sets, and variables of interest, so long as the model archives include sufficient temporal samples. The sensitivities of these statistics were likely reduced by the close developmental relation between the reanalyses and parameterization schemes examined here, so future studies intercomparing more independent schemes may yield even larger and more telling variations.

Acknowledgments. We are grateful for the support received through NOAA Grant NA17RJ1231 and NASA Grants NNG05GR40G and NNG06GC85G. This research was partially supported by an appointment to the NASA Postdoctoral Program at NASA

Goddard Institute for Space Studies, administered by Oak Ridge Associated Universities (ORAU) through a contract with NASA. The views expressed herein are those of the authors and do not necessarily reflect the views of NOAA, NASA, or ORAU. We would also like to thank Masao Kanamitsu and Hideki Kanamaru for modeling advice, as well as Martin Olivera, Jack Ritchie, and Patrick Tripp for technical support.

References

Betts, A. K., J. H. Ball, and P. Viterbo, 1999: Basin-scale surface water and energy budgets for the Mississippi from the ECMWF reanalysis. *J. Geophys. Res.,* **104** (D16), 19 293–19 306.

Ek, M. B., K. E. Mitchell, Y. Lin, E. Rogers, P. Grunmann, V. Koren, G. Gayno, and J. D. Tarpley, 2003: Implementation of Noah land surface model advances in the National Centers for Environmental Prediction operational mesoscale Eta model. *J. Geophys. Res.,* **108,** 8851, doi:10.1029/2002JD003296.

Gates, W. L., and Coauthors, 1999: An overview of the results of the Atmospheric Model Intercomparison Project (AMIP I). *Bull. Amer. Meteor. Soc.,* **80,** 29–55.

Gilman, D. L., F. J. Fuglister, and J. M. Mitchell, 1963: On the power spectrum of "red noise". *J. Atmos. Sci.,* **20,** 182–184.

Kato, H., M. Rodell, F. Beyrich, H. Cleugh, E. van Gorsel, H. Liu, and T. P. Meyers, 2007: Sensitivity of land surface simulations to model physics, land characteristics, and forcings, at four CEOP sites. *J. Meteor. Soc. Japan,* **85,** 187–204.

Kanamitsu, M., W. Ebisuzaki, J. Woollen, S.-K. Yang, J. Hnilo, M. Fiorino, and J. Potter, 2002a: NCEP/DOE AMIP-II Reanalysis (R-2). *Bull. Amer. Meteor. Soc.,* **83,** 1631–1643.

——, and Coauthors, 2002b: NCEP dynamical seasonal forecast system 2000. *Bull. Amer. Meteor. Soc.,* **83,** 1019–1037.

Koike, T., 2004: The Coordinated Enhanced Observing Period—An initial step for integrated global water cycle observation. *WMO Bull.,* **53,** 1–8.

Lawford, R., and Coauthors, 2006: U.S. contributions to the CEOP. *Bull. Amer. Meteor. Soc.,* **87,** 927–939.

Meinke, I., J. Roads, and M. Kanamitsu, 2007: Evaluation of RSM-simulated precipitation during CEOP. *J. Meteor. Soc. Japan,* **85A,** 145–166.

Moorthi, S., and M. J. Suarez, 1992: Relaxed Arakawa–Schubert: A parameterization of moist convection for general circulation models. *Mon. Wea. Rev.,* **120,** 978–1002.

Nigam, S., and A. Ruiz-Barradas, 2006: Seasonal hydroclimate variability over North America in global and regional reanalyses and AMIP simulations: Varied representation. *J. Climate,* **19,** 815–837.

Pan, H.-L., and L. Mahrt, 1987: Interaction between soil hydrology and boundary layer developments. *Bound.-Layer Meteor.,* **38,** 185–202.

——, and W.-S. Wu, 1995: Implementing a mass flux convection parameterization package for the NMC Medium-Range Forecast Model. NMC Office Note 409, 40 pp. [Available from NCEP/EMC, 5200 Auth Road, Camp Springs, MD 20746.]

Roads, J. O., S.-C. Chen, A. K. Guetter, and K. P. Geogakakos, 1994: Large-scale aspects of the United States hydrologic cycle. *Bull. Amer. Meteor. Soc.,* **75,** 1589–1610.

——, ——, M. Kanamitsu, and H. Juang, 1999: Surface water characteristics in NCEP global spectral model and reanalysis. *J. Geophys. Res.,* **104** (D16), 19 307–19 327.

Roads, J., M. Kanamitsu, and R. Stewart, 2002: CSE water and energy budgets in the NCEP–DOE Reanalysis II. *J. Hydrometeor.,* **3,** 227–248.

Ruane, A. C., and J. O. Roads, 2007a: The diurnal cycle of water and energy over the continental United States from three reanalyses. *J. Meteor. Soc. Japan,* **85,** 117–143.

——, and ——, 2007b: 6-hour to 1-year variance of five global precipitation sets. *Earth Interactions,* **11.** [Available online at http://EarthInteractions.org.]

——, and ——, 2008: Dominant balances and exchanges of the atmospheric water cycle in the Reanalysis-2 at diurnal, annual, and intraseasonal time scales. *J. Climate,* in press.

Schubert, S., and Y. Chang, 1996: An objective method for inferring sources of model error. *Mon. Wea. Rev.,* **124,** 325–340.

Trenberth, K. E., and C. J. Guillemot, 1998: Evaluation of the atmospheric moisture and hydrologic cycle in the NCEP/NCAR reanalyses. *Climate Dyn.,* **14,** 213–231.

——, A. Dai, R. M. Rasmussen, and D. B. Parsons, 2003: The changing character of precipitation. *Bull. Amer. Meteor. Soc.,* **84,** 1205–1217.

Wu, W., and R. E. Dickinson, 2004: Time scales of layered soil moisture memory in the context of land–atmosphere interaction. *J. Climate,* **17,** 2752–2764.

Earth Interactions is published jointly by the American Meteorological Society, the American Geophysical Union, and the Association of American Geographers. Permission to use figures, tables, and *brief* excerpts from this journal in scientific and educational works is hereby granted provided that the source is acknowledged. Any use of material in this journal that is determined to be "fair use" under Section 107 or that satisfies the conditions specified in Section 108 of the U.S. Copyright Law (17 USC, as revised by P.IL. 94-553) does not require the publishers' permission. For permission for any other form of copying, contact one of the copublishing societies.